

# Prior to Segment: Foreground Cues for Novel Objects in Partially Supervised Instance Segmentation

David Biertimpel<sup>1,2\*</sup> Sindi Shkodrani<sup>2</sup> Anil S. Baslamisli<sup>1</sup> Nóra Baka<sup>2</sup>

<sup>1</sup>University of Amsterdam <sup>2</sup>TomTom

david.biertimpel@protonmail.com a.s.baslamisli@uva.nl

{sindi.shkodrani, nora.baka}@tomtom.com

## Abstract

Instance segmentation methods require large datasets with expensive instance-level mask labels. This makes partially supervised learning appealing in settings where abundant box and limited mask labels are available. To improve mask predictions with limited labels, we modify a Mask R-CNN by introducing an object mask prior (OMP) for the mask head. We show that a conventional class-agnostic mask head has difficulties learning foreground for classes with box-supervision only. Our OMP resolves this by providing the mask head with the general concept of foreground implicitly learned by the box classification head under the supervision of all classes. This helps the class-agnostic mask head to focus on the primary object in a region of interest (RoI) and improves generalization to novel classes. We test our approach on the COCO dataset using different splits of strongly and weakly supervised classes. Our approach significantly improves over the Mask R-CNN baseline and obtains competitive performance with the state-of-the-art, while offering a much simpler architecture. <sup>1</sup>

## 1. Introduction

Instance segmentation is an essential task in computer vision with applications ranging from autonomous vehicles to robotics and medical imaging [5, 6, 14, 22, 26, 30]. A major contributor to the success of recent instance segmentation methods is the availability of the large-scale datasets with numerous instance-level mask labels [7, 8, 12, 24, 33]. The problem with the mask labels is that their acquisition is rather time-consuming. A single instance mask takes around 67 seconds to annotate, which is on average  $\sim 6.5x$  longer than drawing a bounding box, and  $\sim 67x$  longer than identifying image-level labels [4]. As a result, only a small

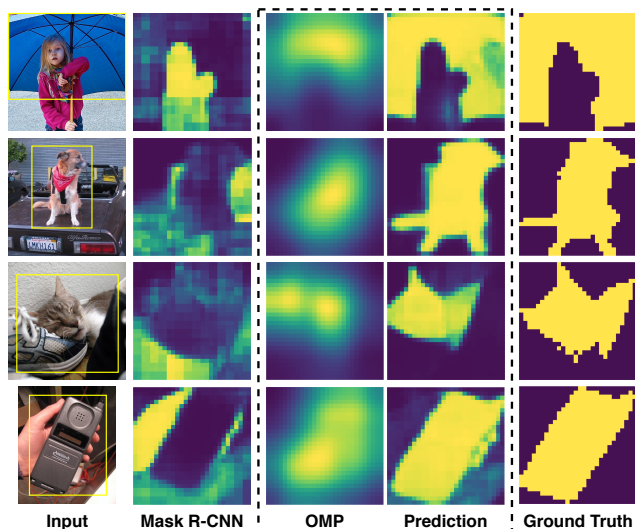


Figure 1: Our object mask prior (OMP) provides foreground cues to the mask head highlighting the primary instance in ambiguous RoIs. OPMask is able to resolve ambiguous constellations and segment the correct instance, while the Mask R-CNN baseline fails to do so.

subset of computer vision data is instance mask annotated. While mask labels are expensive and scarce, bounding box labels are quicker to annotate and more abundant.

Therefore, recent research focuses on approaching the problem in a partially supervised learning setting [9, 17, 20, 38], where all instance classes (*i.e.* categories) are box annotated, but only a subset of the classes carry instance mask labels. The goal is to predict instance masks for *novel* classes for which only box labels are available (*i.e.* novel for the mask head). For novel classes, conventional methods perform poorly and tend to generate mask predictions that are perforated, not covering the entire object or completely missing it [17, 20].

\*This paper is the product of work during an internship at TomTom.

<sup>1</sup>Code is available at: [github.com/dbtimp/OPMask](https://github.com/dbtimp/OPMask)

The task of generalizing to novel classes is either achieved with meta-learning of class aware weights [17] or with a class agnostic mask head [9, 20, 38]. In the latter case, instead of predicting a mask per class, each pixel in the RoI is classified into either foreground or background. The class agnostic mask head faces the challenge of having to learn a general concept of foreground in order to generalize to unseen object classes. This often fails, even if abundant box labels are provided for the novel class.

In this paper, we identify that the problem originates, on the one hand, from the ambiguous constellations between object instances, where pixels of one instance appear in the bounding box of the other. Thus, the actual foreground becomes ambiguous to the mask head when the RoI contains multiple and possibly overlapping instances. See Figure 1 for examples. On the other hand, instances of novel classes that appear in the background of a RoI during training are actively learned as background. This hurts generalization to novel classes that frequently interact with other supervised classes. To address these problems, we introduce an object mask prior (OMP) that highlights the correct foreground in each RoI. This helps the mask head to resolve ambiguous constellations, learn a more general concept of the foreground, and generalize it to novel classes.

Recent works have demonstrated that shape priors are beneficial inductive biases that steer the models towards more stable mask predictions. For example, ShapeMask [20] creates a knowledge base of shape priors by applying k-means to the ground-truth masks, whereas ShapeProp [38] creates the priors by using pixel-wise multiple instance learning on bounding boxes. Although these priors help to generalize to novel classes, they still suffer from the problems mentioned above as they do not model a general concept of foreground or do not address ambiguous RoIs.

Conversely, our prior is explicitly optimized to highlight the foreground in a RoI using the box supervision from all classes. This is achieved by exploiting the fact that the box classification head naturally learns to identify the primary class in a RoI. As the box head receives labels for all classes in the partially supervised setting, the box features capture a general concept of foreground. To reveal this foreground, we use class activation maps (CAMs) [37], which are coarse localization maps indicating the most discriminative image regions detected by the model. Therefore, given a correct classification, CAMs are expected to highlight foreground areas corresponding to the primary RoI class.

Unlike other methods that introduce separate modules for prior creation, we natively embed the OMP into our model in an end-to-end manner, without introducing any architectural overhead. Besides using box supervision from all classes, our prior is able to utilize mask gradients originated from the limited mask labels to increase its spatial extent, without needing any separate refinement modules.

We embed our OMP in the Mask R-CNN meta architecture and name our overall model OPMask (Object Prior Mask R-CNN). Our main contributions are the following:

- We identify two fundamental problems in partially supervised instance segmentation: First, instances of novel classes appearing in the background of a mask supervised RoI during training are learned as background by the model. Second, in ambiguous RoIs containing multiple and possibly overlapping instances, the mask head has difficulties finding the foreground.
- We introduce an object mask prior (OMP) in the mask head to solve the above identified problems. The prior highlights the foreground across all classes by leveraging the information from the box head.
- On COCO dataset [24], OPMask significantly improves over our Mask R-CNN baseline by 13.0 AP. Compared with the prior state-of-the-art, we improve over ShapeMask [20] and ShapeProp [38] and achieve competitive results against CPMask [9] while using a much simpler architecture.

Finally, we identify the problem of overfitting in the mask head when training with a schedule optimized for the fully supervised task. We address this issue by crafting a better schedule for the task at hand.

## 2. Related Work

**Instance segmentation** aims to segment every object instance in a scene. Detection based approaches [6, 14, 22, 26], which add a mask prediction network to existing detection models, represent the current state of the art. Mask R-CNN [14] extends the two stage detection network Faster R-CNN [31] being the first to introduce a multi-task loss combining detection and mask gradients. Mask R-CNN is a strong baseline and often used as a meta-architecture due to its extensibility. Contour based approaches [27, 30, 35] segment objects by refining a sequence of vertices to match the object shape. Bottom-up approaches group pixels to generate instance masks [2, 25, 28]. As these approaches need large datasets with pixel-wise supervision, they are not suited for the partially supervised task.

**Partially supervised instance segmentation.** In partially supervised instance segmentation, a subset of classes is strongly annotated with box and mask supervision, while the remaining classes carry only weak box labels. The goal is to use the box labels in conjunction with the limited masks to predict instance masks for all classes.

The pioneering approach by Hu *et al.* [17] augments a Mask R-CNN with a weight transfer function that learns a mapping from box to mask weights, introducing a class aware mask head capturing a representation for all classes.

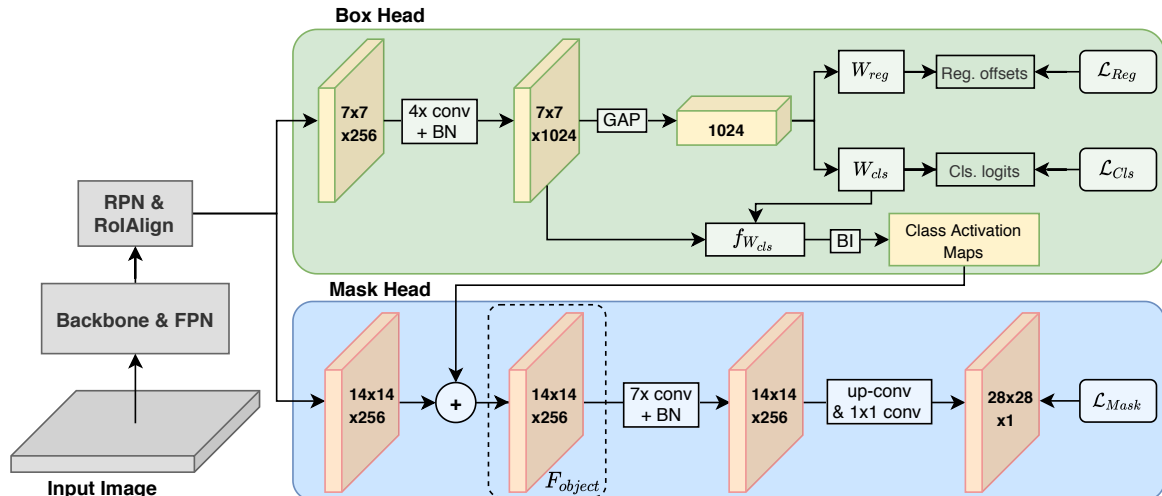


Figure 2: Overall architecture. The box head generates our OMP which is added to features entering the mask head to create object aware features  $F_{object}$ . The mask head then uses  $F_{object}$  to predict instance masks.

Kuo *et al.* introduce ShapeMask [20] that creates a knowledge base of shape priors by applying k-means to the available ground-truth masks. A box embedding, gives rise to a linear combination of the k-means centroids generating a shape prior that is further refined into an instance mask. ShapeMask bases its prior solely on the limited mask labels. In contrast, we use box labels of all available classes and use mask labels for refinement.

ShapeProp [38] uses pixel-wise multiple instance learning (MIL) on bounding boxes to create a saliency heatmap, which is further processed leading to a more expressive shape activation map. Both ShapeProp and OPMask utilize box labels to generate a prior for mask prediction. ShapeProp introduces two separate modules to generate and refine their prior. On the other hand, we take advantage of the fact that the box head implicitly learns a concept of foreground. Thus, we design our model to leverage the features that are already made available by the box head. This way we do not introduce any architectural overhead.

Finally, Fan *et al.* [9] learn the underlying shape and appearance commonalities between instance masks that should generalize to novel classes. The shape commonalities are learned by a boundary prediction head, while the appearance commonalities are enforced by an attention based affinity parsing module. Besides learning commonalities that aid generalization, we also identify that a major problem lies in ambiguous RoIs and the mask head having difficulties to learn a general concept of foreground. To address this, we utilize our OMP, which highlights the foreground of a RoI to resolve ambiguous constellations and help generalize to novel classes.

**Weakly supervised instance segmentation** approaches solely rely on weak labels such as bounding boxes or images level labels [1, 3, 10, 16, 19, 21, 39, 40]. Models using image-level labels [1, 10, 21, 39, 40] mostly use CAM based image-wide localization information to assist instance mask prediction. Zhou *et al.* [39] use the peaks of a class response map to detect and segment instances. Ge *et al.* [10] refine object attention maps using multi-task network heads sharing the same backbone. Both Laradji *et al.* [21] and Ahn *et al.* [1] create and refine pseudo masks which are later used to train a Mask R-CNN [14]. Setups where only image-level labels are available require the introduction of complex refinement modules. Conversely, in our setting, we rely on mask gradients that are already available in the model to improve our OMP.

Less work has been done using box supervision [16, 19]. Hsu *et al.* [16] employ a Mask R-CNN like architecture, where the mask head uses a MIL objective. Khoreva *et al.* [19] uses GrabCut [32] to create pseudo ground truths to train a separate segmentation model. Instead of using box pixels to predict masks, we use CAMs to extract the foreground information in the box features to create our OMP.

### 3. Method

In partially supervised instance segmentation, a conventional Mask R-CNN with a class agnostic mask head fails to predict reliable instance masks for certain novel classes, as demonstrated in Figures 1 and 4, and as discussed in the introduction. To address this, we propose OPMask which introduces an object mask prior (OMP) that captures foreground cues for all classes in the dataset (i.e. generalized

foreground). OPMask follows the design of a Mask R-CNN [14] with a ResNet [15] backbone equipped with FPN [23]. The model is illustrated in Figure 2.

### 3.1. Object Mask Prior (OMP)

The OMP functions as an inductive bias capturing a general concept of foreground to improve generalization to novel classes. In the partially supervised learning setup, predicting a general foreground is non-trivial for two main reasons: (1) pixel-wise mask labels are missing for a subset of classes, (2) in many cases RoIs contain multiple and overlapping instances, making the foreground in a RoI ambiguous. The OMP tackles these issues by highlighting the correct foreground in each RoI, which helps the mask head to learn a more general concept of the foreground, resolve ambiguous RoIs, and generalize it to novel classes.

We create such a prior by extracting the foreground information captured by the box features in the box head. We use the fact that the box classification head learns a representation of the primary class (*i.e.* foreground) for all classes in the dataset. To reveal this foreground, we use class activation maps (CAMs) [37], which provide coarse localization maps emphasizing the most discriminative regions the model uses for classification. Consequently, given a correct classification, CAMs are expected to highlight foreground areas corresponding to the primary RoI class.

To enable CAM calculation, we use a box head with four convolution layers where Global Average Pooling (GAP) is applied on the last convolutional feature map. The resulting vector is processed by linear layers for box classification and regression (see Figure 2). We calculate CAMs with a function  $f_{W_{cls}}$  which is a  $1 \times 1$  convolution parameterized with the classification weights  $W_{cls}$  as follows:

$$M_{cam} = f_{W_{cls}}(F_{box}), \quad (1)$$

where  $F_{box}$  is the last feature map of the box head before GAP. This allows calculating all CAMs efficiently with a single operation while keeping them differentiable. Depending on whether it is training or inference time, we use the ground truth labels or the classes predicted by the box head to select the correct CAM slice from  $M_{cam}$ .

The CAMs of the correct class are added to the corresponding mask features as will be described in the next section. Apart from providing the mask head favorable foreground cues, this also allows the mask gradients backpropagate through the box head. A well known shortcoming of CAMs is that they do not cover the full extent of the objects, but only the minimal area of the most distinctive features. The mask gradients provide the features in the box head mask information, which leads to an increase in the spatial extent of the CAMs allowing them to capture finer details.

As a result, CAMs that receive mask gradients give rise to our OMP. The fact that the OMP originates from the box

classification task, which is directly optimized to classify the primary instance in a RoI, provides it with strong foreground cues. This makes our OMP predestined to provide our mask head with a general concept of foreground allowing it to resolve ambiguous RoIs and also better generalize to novel classes.

### 3.2. Integrating the Prior

After generating the OMP, we aggregate it with the FPN features after the RoIAlign  $F_{fpn}$  to create object-aware features  $F_{object}$  as follows:

$$F_{object} = F_{fpn} + M_{cam}, \quad (2)$$

where  $M_{cam,k} \in \mathbb{R}^{H,W}$  is added to each channel of its matching RoI  $F_{fpn,k} \in \mathbb{R}^{D,H,W}$ . Before addition, we use bilinear interpolation to adjust  $M_{cam}$  to the spatial dimensions of  $F_{fpn}$ .

The addition leads to a mean shift in  $F_{fpn}$  emphasizing the features corresponding to the areas highlighted by the OMP. This incentivizes the mask head to learn a general concept of foreground for all classes in the dataset.

Afterwards,  $F_{object}$  is processed by a function  $f_{mask}$  consisting of seven  $3 \times 3$  convolution layers followed by one transposed convolution layer doubling the features spatial resolution and one  $1 \times 1$  convolution performing mask prediction as follows:

$$M_{mask} = f_{mask}(F_{object}), \quad (3)$$

where  $M_{mask}$  is the mask prediction after applying a pixel-wise sigmoid. We use seven convolution layers to achieve a receptive field large enough such that  $f_{mask}$  operates on the the entire input feature map. Batch normalization [18] is applied after each  $3 \times 3$  convolution to utilize its stochastic properties to improve generalization. Finally, a pixel-wise binary cross-entropy loss is applied to  $M_{mask}$  using the available mask labels  $M_{gt}$  as follows:

$$\mathcal{L}_{Mask} = BCE(M_{mask}, M_{gt}). \quad (4)$$

## 4. Experiments

In Section 4.1 we introduce the dataset and experimental setup. In Section 4.2, we provide evidence that instances of novel classes appearing in the background of a RoI during training are learned as background, and a conventional class agnostic mask head has difficulties considering the correct foreground in ambiguous RoIs. Then, Section 4.3, shows the capabilities of OPMask to generalize to novel classes. In Section 4.4, we compare our OMP against regular CAMs showing the positive impact of mask gradients updating box features. Finally, in Section 4.5, we discuss an inherent optimization conflict between box and mask head and introduce a new training schedule that reduces overfitting.

## 4.1. Experimental Setup

We conduct our experiments on the COCO dataset [24]. To realize the partially-supervised learning setup, we split the mask labels of the 80 COCO *thing* classes into two subsets. One subset is used for training, one for evaluation and vice versa. Box labels are available for all classes during training. To compare against related work, we mainly focus on dividing between the 20 classes of the Pascal voc dataset [8], and the remaining 60 unique COCO classes. During training we use SGD with Momentum with an initial learning rate of 0.02 which we linearly warmup for the first 1000 iterations [11]. The image batch size is 16 and we stabilize gradients by clipping them at a value of 1.0. For all models we use the 130k training schedule introduced in Section 4.5. As a backbone we use ResNet-50 and ResNet-101 [15] with a FPN [23]. Our implementation is based on PyTorch [29] and Detectron2 [34]. For further details please refer to appendix A.

## 4.2. Insights on Identifying Foreground in RoIs

**Learning classes as background.** A class agnostic mask head faces the task of classifying RoI pixels between foreground or background, where pixels that correspond to supervised classes are considered foreground, while all other pixels are regarded as background. The COCO dataset contains complex scenes with cluttered objects, which causes RoIs to often contain more than one instance. Background pixels can either be part of the available supervised classes, belong to novel classes to which we want to generalize, or not be part of any class in the dataset. In the second case, we face the dilemma that the model actively learns to classify features that correspond to novel classes as background. This clearly conflicts with the generalization goal of the partially supervised learning task.

This phenomenon particularly affects classes that frequently interact with other classes and thus appear more often in the background of a mask supervised RoI. To investigate this, we compute the correlation between class overlap and mask AP for novel classes (in voc  $\rightarrow$  non-voc and non-voc  $\rightarrow$  voc). To approximate the overlap between classes we compute the IoU of all ground-truth bounding boxes in the COCO dataset. Afterwards, we compute a regression between the mean IoU of each class and its mask AP.

Two regression models are presented in Figure 3. The first (*left*) is computed with our Mask R-CNN baseline showing a significant negative correlation between mean IoU and mask AP across all classes ( $p = .003 < .01$ ). This provides evidence for our hypothesis that novel classes appearing in the background of RoIs are actively learned as background during training. The second regression (*right*), computed with OPMask, shows only a weak negative correlation that is not strong enough to reach significance ( $p = .189 \not< .01$ ). At the same time, we see notable improve-

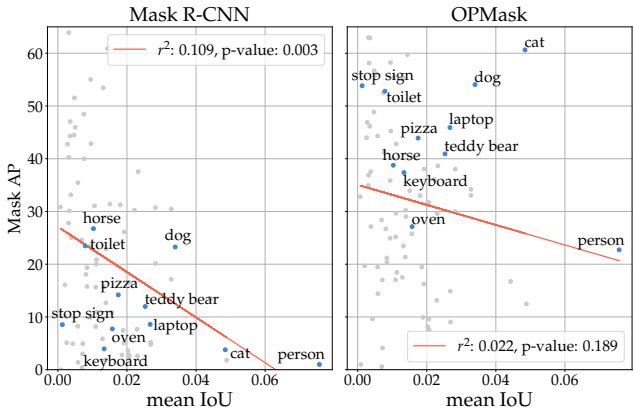


Figure 3: Regression showing the correlation between box IoU and mask AP of all classes in COCO. We compare the mask AP scores of achieved with our Mask R-CNN baseline (*left*) and OPMask (*right*). The classes with the largest relative improvement are highlighted.

ments for classes with high mean IoU values, which are more likely to appear in the background of other classes RoIs (*e.g.* *person*: 0.99 to 22.72 AP, *cat*: 3.77 to 60.63 AP). This suggests that our OMP is able to provide the mask head with a general concept of foreground, which counteracts learning these novel classes as background.

**Resolving ambiguous RoIs.** Another problem with multiple and possibly overlapping instances is that the primary instance (*i.e.* foreground) of the RoI is ambiguous. A conventional mask head has difficulties to locate the foreground in these constellations. This applies particularly to the partially supervised learning setup, as the mask head is inclined to consider the supervised classes as foreground and disregard unseen classes.

Figure 1 presents a number of ambiguous RoIs where a Mask R-CNN with a class agnostic mask head falsely predicts background instances as foregrounds. On the other hand, notice how the OMP is able to highlight the foreground instance allowing OPMask to make a correct mask prediction. It can also be observed that it is sufficient for the OMP to provide a coarse foreground cue to enable precise mask predictions. All examples are from models trained either in the voc  $\rightarrow$  non-voc or non-voc  $\rightarrow$  voc setting. Interestingly, the results in the first row are achieved with models trained where *person* is a supervised class and *umbrella* a novel class. While the Mask R-CNN incorrectly segments the *person*, OPMask identifies the *umbrella* as the primary class and is able to predict an accurate instance mask.

## 4.3. Generalization to Novel Classes

**Baseline.** We use a Mask R-CNN with a class agnostic mask head. For a fair comparison, we use the same box

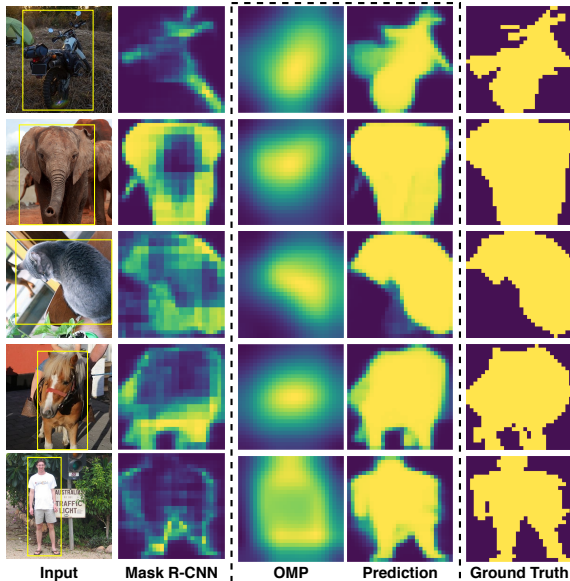


Figure 4: The Mask R-CNN baseline produces perforated, incomplete or missing masks. OPMask driven by the OMP is able to accurately segment each novel object.

head as OPMask and also add batch norm to its mask head. In Table 1 we call this baseline ‘Our Mask R-CNN’.

**Pascal voc vs. non-voc classes.** We present the quantitative results for the voc vs. non-voc splits in Table 1. First, we notice that OPMask considerably improves over our Mask R-CNN baseline in all cases. For example, with ResNet-50 backbone, a significant increase of 10.1 AP in non-voc  $\rightarrow$  voc and 13.0 AP in voc  $\rightarrow$  non-voc is achieved. OPMask also performs better than previous approaches ShapeProp [38] and ShapeMask [20] in all cases. It is notable that even with a ResNet-50, we achieve better or competitive performance than ShapeMask and ShapeProp that are equipped with the stronger ResNet-101. When comparing OPMask with the recently released CPMask [9], we observe competitive performance in non-voc  $\rightarrow$  voc (e.g. increase of 0.3 AP), but also slightly worse performance in voc  $\rightarrow$  non-voc (e.g. 0.8 AP decrease). It should be noted, however, that unlike us, CPMask uses multi-scale training, which leads to general performance improvements. We also emphasize that OPMask has a much simpler architecture than all of our related work.

**Qualitative Results.** In Figures 1 and 4, we provide qualitative insights into how our OMP steers mask prediction and improves generalization to novel classes. Each example shows a novel class in either the voc  $\rightarrow$  non-voc or non-voc  $\rightarrow$  voc setup. Next to the OMP and mask prediction of OPMask, our Mask R-CNN baseline predictions are presented. The results show that the OMPs properly identify and highlight the primary RoI instances while covering

most of the objects’ spatial extent. Furthermore, we realize that our coarse prior is sufficient to enable the mask head to generalize to a refined mask. This underlines our hypothesis that it is of particular importance to provide the class agnostic mask head with a general concept of foreground across all classes. Finally, Figure 5 presents a number of COCO images with overlaid mask predictions produced in the voc  $\rightarrow$  non-voc setup. The results show OPMask’s ability to generate precise predictions for novel objects across different scenarios and object sizes. All examples in this section are achieved with models equipped with a ResNet-101.

**Strongly vs weakly supervised class ratios.** To provide a better overview of OPMask’s generalization abilities we evaluate the performance on different class splits. In Figure 6, it can be observed that OPMask remains stable across all class splits and consistently improves over our Mask R-CNN baseline. To create the 40 class split, we start with 20 Pascal voc [8] classes and randomly add another 20 classes from the non-voc split. We also observe improvements of 1.6 AP when training on all COCO classes. We consider that these improvements can be attributed to the OMP helping the class agnostic mask head to resolve ambiguous RoIs. Overall, the results show that the OMP makes predictions of supervised classes more reliable and precise.

#### 4.4. Refining the Object Mask Prior

A simple CAM as the OMP would do a reasonable job, though a better prior leads to a better segmentation result. To improve our OMP, we let mask gradients backpropagate through the box head, which augments the box features with mask information. This causes the CAMs to increase their spatial extent, allowing our OMP to cover larger parts of the objects, improving the final mask AP by 1.1 points in non-voc  $\rightarrow$  voc with ResNet-50 backbone. To further investigate the improvement of the prior, we compare the mask AP of our OMP with vanilla CAMs on the COCO validation set. We compare against a Faster R-CNN and a Mask R-CNN with the same box head as OPMask. In Table 2, AP and AP<sub>50</sub> results of voc vs. non-voc class splits are provided. Since the Faster R-CNN does not receive any mask gradients it is only trained and evaluated on all classes.

The results show that our OMP is significantly better than the CAMs of Faster R-CNN and Mask R-CNN. This underlines the positive influence of mask gradients on box head features and consequently on our OMP. The low AP values of the CAMs generated by Faster R-CNN and Mask R-CNN are caused by the fact that they often do not surpass the pixel-wise IoU threshold (i.e.  $\geq 0.5$ ) and are mostly considered negatives. The Mask R-CNN, where the backbone features are augmented with mask gradients, does not show significant improvements over the Faster R-CNN. This suggests that for CAM refinement, mask gradients should impact the features that are directly used to cal-

Backbone	Method	non-voc $\rightarrow$ voc: test on voc						voc $\rightarrow$ non-voc: test on non-voc					
		AP	AP <sub>50</sub>	AP <sub>75</sub>	AP <sub>S</sub>	AP <sub>M</sub>	AP <sub>L</sub>	AP	AP <sub>50</sub>	AP <sub>75</sub>	AP <sub>S</sub>	AP <sub>M</sub>	AP <sub>L</sub>
R-50-FPN	Mask R-CNN [14]	23.9	42.9	23.5	11.6	24.3	33.7	19.2	36.4	18.4	11.5	23.3	24.4
	Our Mask R-CNN	26.4	46.4	26.7	14.2	26.4	36.5	18.9	35.5	18.4	12.4	22.8	22.9
	Mask <sup>X</sup> R-CNN [17]	28.9	52.2	28.6	12.1	29.0	40.6	23.7	43.1	23.5	12.4	27.6	32.9
	Mask R-CNN w/ ShapeProp [38]	34.4	59.6	35.2	13.5	32.9	48.6	30.4	51.2	31.8	14.3	34.2	44.7
	<b>OPMask</b>	<b>36.5</b>	<b>62.5</b>	<b>37.4</b>	<b>17.3</b>	<b>34.8</b>	<b>49.8</b>	<b>31.9</b>	<b>52.2</b>	<b>33.7</b>	<b>16.3</b>	<b>35.2</b>	<b>46.5</b>
R-101-FPN	Mask R-CNN [14]	24.7	43.5	24.9	11.4	25.7	35.1	18.5	34.8	18.1	11.3	23.4	21.7
	Our Mask R-CNN	27.7	48.0	28.2	13.6	28.6	38.0	21.0	39.2	20.5	13.5	26.4	23.9
	Mask <sup>X</sup> R-CNN [17]	29.5	52.4	29.7	13.4	30.2	41.0	23.8	42.9	23.5	12.7	28.1	33.5
	ShapeMask [20]	33.3	56.9	34.3	17.1	38.1	45.4	30.2	49.3	31.5	16.1	38.2	28.4
	Mask R-CNN w/ ShapeProp [38]	35.5	60.5	36.7	15.6	33.8	50.3	31.9	52.1	33.7	14.2	35.9	46.5
	CPMask [9]	36.8	60.5	<b>38.6</b>	<b>17.6</b>	<b>37.1</b>	<b>51.5</b>	<b>34.0</b>	<b>53.7</b>	<b>36.5</b>	<b>18.5</b>	<b>38.9</b>	<b>47.4</b>
	<b>OPMask</b>	<b>37.1</b>	<b>62.5</b>	38.4	16.9	36.0	50.5	33.2	53.5	35.2	17.2	37.1	46.9

Table 1: Comparing OPMask with the state-of-the-art in the partially supervised instance segmentation setup on COCO. non-voc  $\rightarrow$  voc signifies that the mask head receives supervision from the non-voc classes and is tested on voc classes, vice versa the same applies to voc  $\rightarrow$  non-voc.

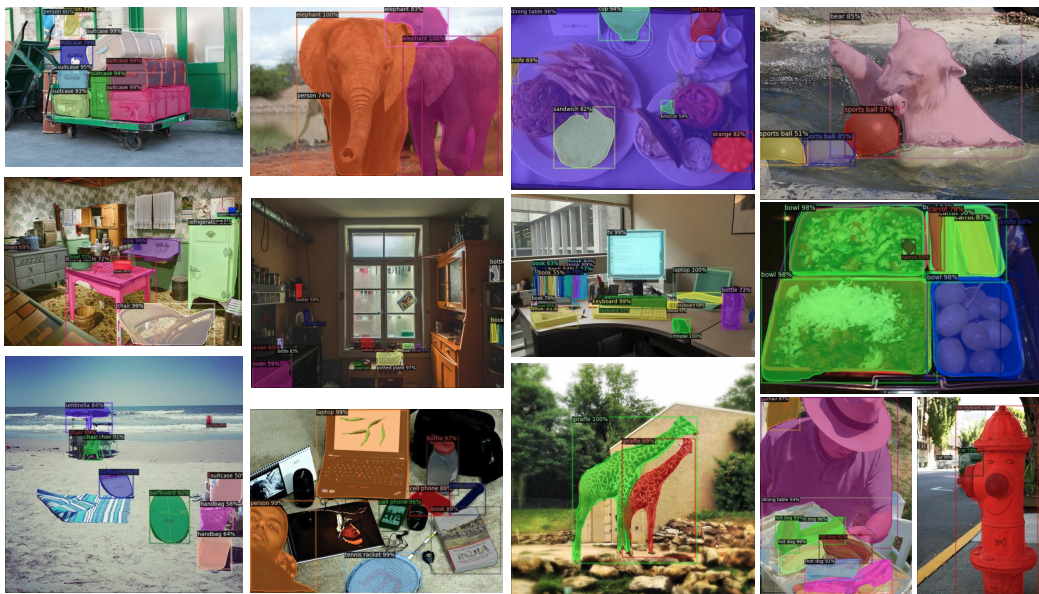


Figure 5: Qualitative results on COCO using the voc  $\rightarrow$  non-voc split for training. This shows the ability of OPMask to predict precise instance masks for novel objects across different scenes, and various object sizes and appearances.

culate the activations. Finally, Figure 7 demonstrates qualitative improvements of CAMs on different COCO images.

#### 4.5. Introducing a New Training Schedule

When training with conventional schedules optimized for fully supervised setups [13, 34], we observed considerable overfitting of the mask head. We argue that this indicates a fundamental challenge in the partially supervised learning task, where the box head receives labels for all classes (and performs optimal with a training schedule for a fully supervised setup), while the mask head can only access a subset of the labels (and thereby might overfit easier).

Indeed, after the second learning rate step of a usual Mask R-CNN schedule [34], the mask head overfits to the supervised classes and generalizes worse. To address this issue, we craft a new schedule that introduces a better compromise between box and mask performance.

For this, we randomly sampled a separate validation set from the COCO training set of the same size as the regular validation set (*i.e.* 5000 images). We then trained OPMask for 180k iterations with one learning rate step after 120k iterations. To determine the new schedule, we selected the iteration with the model that performed best on the novel classes, selecting the best compromise between the voc vs.

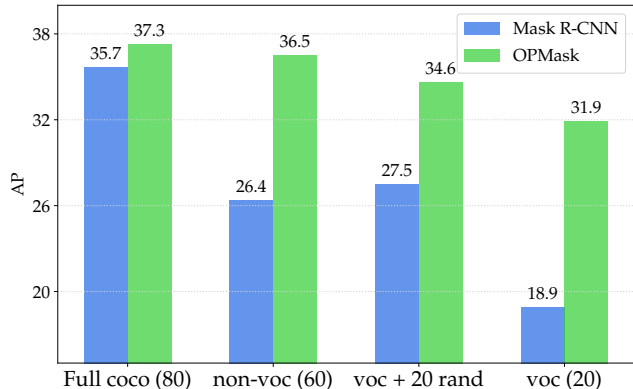


Figure 6: Performance of OPMask on varying numbers of supervised classes. OPMask significantly improves over our Mask R-CNN baseline across all class splits, including the fully supervised setup.

Model	train set	test on all		test on voc		test on non-voc	
		AP	AP <sub>50</sub>	AP	AP <sub>50</sub>	AP	AP <sub>50</sub>
Faster R-CNN	all	0.2	1.0	0.3	2.5	0.1	0.6
Mask R-CNN	all	0.2	1.3	0.3	2.3	0.1	1.0
Mask R-CNN	voc	0.3	1.9	0.6	4.0	0.2	1.0
Mask R-CNN	non-voc	0.2	1.5	0.4	2.8	0.2	1.0
OPMask	all	8.8	34.1	9.9	40.4	8.4	32.0
OPMask	voc	5.0	21.8	9.9	38.5	3.3	16.3
OPMask	non-voc	8.0	31.5	7.0	32.2	8.3	31.2

Table 2: Quantitative comparison of our OMP with CAMs produced by a Faster R-CNN and Mask R-CNN. The results show that our OMP covers much larger parts of the objects than conventional CAMs.

non-voc splits. This resulted in a new schedule of 130k iterations with a learning rate step after 120k iterations.

Backbone	lr sched.	non-voc $\rightarrow$ voc		voc $\rightarrow$ non-voc	
		AP <sub>Box</sub>	AP	AP <sub>Box</sub>	AP
R-50-FPN	1x	39.3	35.2	39.3	29.0
	130k	39.6	36.5	39.8	<b>31.9</b>
	3x	<b>41.7</b>	<b>36.7</b>	<b>41.8</b>	31.1
R-101-FPN	130k	41.1	37.1	41.7	<b>33.2</b>
	3x	<b>43.2</b>	<b>38.2</b>	<b>43.4</b>	32.7

Table 3: Comparing our 130k schedule with the popular 1x and 3x schedules in the partially supervised learning setup. AP<sub>Box</sub> and AP denote box and mask AP, respectively.

In Table 3, we compare OPMask trained with the new 130k schedule with the conventional 1x and 3x schedules [13, 34] optimized for the fully supervised setup. The box head, which receives supervision for all classes, performs best with the 3x schedule (see AP<sub>Box</sub>). In contrast, the mask head, receiving only labels for a subset of the classes, shows

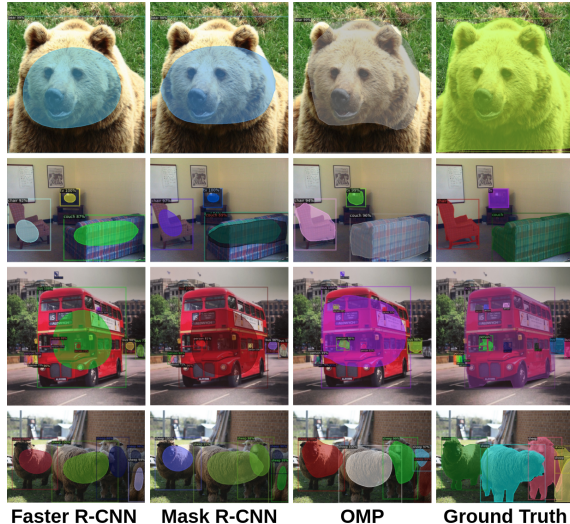


Figure 7: Comparing our OMP with CAMs from a Faster R-CNN and Mask R-CNN on COCO images. Our OMP is able to cover much more of the objects than regular CAMs.

a different behavior. In the voc  $\rightarrow$  non-voc split, our 130k schedule performs considerably better than the 3x schedule despite worse AP<sub>Box</sub>. With more mask labels available (non-voc  $\rightarrow$  voc) the effect is not as severe, but still notable when considering AP<sub>Box</sub> and mask AP. We emphasize that the mask AP is heavily positively correlated with AP<sub>Box</sub>, as the quality of the instance mask strongly depends on the previously detected box [36]. To this end, our 130k schedule provides a reasonable compromise between AP<sub>Box</sub> and mask AP, which improves cases with less available training data while not sacrificing much performance when more supervision is available.

## 5. Conclusion

We proposed OPMask, a novel approach to partially supervised instance segmentation. OPMask introduces an object mask prior (OMP) that helps its class agnostic mask head to learn a general concept of foreground, resolve ambiguous RoIs and generalize to novel classes. Our research points out two major problems hindering a class agnostic mask head to generalize to novel classes. First, instances of novel classes appearing in the background of a mask supervised RoI during training are learned as background by the model. Second, in ambiguous RoIs that contain multiple and possibly overlapping instances, the mask head has difficulties to consider the correct foreground. We demonstrated that both problems can be vastly alleviated with our OMP that highlights foreground across all classes by leveraging the information from the box head. Finally, we showed that OPMask significantly improves over our Mask R-CNN



baseline and achieves competitive performance with the state-of-the-art, while offering a much simpler architecture.

## References

- [1] Jiwoon Ahn, Sunghyun Cho, and Suha Kwak. Weakly supervised learning of instance segmentation with inter-pixel relations. In *Proceedings of the IEEE/CVF Conference on Computer Vision and Pattern Recognition (CVPR)*, June 2019. 3
- [2] Anurag Arnab and Philip HS Torr. Pixelwise instance segmentation with a dynamically instantiated network. In *Proceedings of the IEEE Conference on Computer Vision and Pattern Recognition*, pages 441–450, 2017. 2
- [3] Aditya Arun, C. V. Jawahar, and M. Pawan Kumar. Weakly supervised instance segmentation by learning annotation consistent instances. In *ECCV*, 2020. 3
- [4] Amy Bearman, Olga Russakovsky, Vittorio Ferrari, and Li Fei-Fei. What’s the point: Semantic segmentation with point supervision. In Max Welling, Nicu Sebe, Jiri Matas, and Bastian Leibe, editors, *Computer Vision - 14th European Conference, ECCV 2016, Proceedings*, Lecture Notes in Computer Science (including subseries Lecture Notes in Artificial Intelligence and Lecture Notes in Bioinformatics), pages 549–565, Germany, 2016. Springer Verlag. 1
- [5] Hao Chen, Kunyang Sun, Zhi Tian, Chunhua Shen, Yongming Huang, and Youliang Yan. Blendmask: Top-down meets bottom-up for instance segmentation. In *Proceedings of the IEEE/CVF Conference on Computer Vision and Pattern Recognition*, pages 8573–8581, 2020. 1
- [6] Tianheng Cheng, Xinggang Wang, Lichao Huang, and Wenyu Liu. Boundary-preserving mask r-cnn. In Andrea Vedaldi, Horst Bischof, Thomas Brox, and Jan-Michael Frahm, editors, *Computer Vision – ECCV 2020*, pages 660–676, Cham, 2020. Springer International Publishing. 1, 2
- [7] M. Cordts, M. Omran, S. Ramos, T. Rehfeld, M. Enzweiler, R. Benenson, U. Franke, S. Roth, and B. Schiele. The cityscapes dataset for semantic urban scene understanding. In *2016 IEEE Conference on Computer Vision and Pattern Recognition (CVPR)*, pages 3213–3223, 2016. 1
- [8] Mark Everingham, Luc Gool, Christopher K. Williams, John Winn, and Andrew Zisserman. The pascal visual object classes (voc) challenge. *Int. J. Comput. Vision*, 88(2):303–338, June 2010. 1, 5, 6
- [9] Qi Fan, Lei Ke, Wenjie Pei, Chi-Keung Tang, and Yu-Wing Tai. Commonality-parsing network across shape and appearance for partially supervised instance segmentation. In *ECCV*, 2020. 1, 2, 3, 6, 7
- [10] Weifeng Ge, Sheng Guo, Weilin Huang, and Matthew R Scott. Label-penet: Sequential label propagation and enhancement networks for weakly supervised instance segmentation. In *Proceedings of the IEEE International Conference on Computer Vision*, pages 3345–3354, 2019. 3
- [11] Priya Goyal, Piotr Dollár, Ross Girshick, Pieter Noordhuis, Lukasz Wesolowski, Aapo Kyrola, Andrew Tulloch, Yangqing Jia, and Kaiming He. Accurate, large mini-batch sgd: Training imagenet in 1 hour. *arXiv preprint arXiv:1706.02677*, 2017. 5
- [12] Agrim Gupta, Piotr Dollar, and Ross Girshick. Lvis: A dataset for large vocabulary instance segmentation. In *Proceedings of the IEEE Conference on Computer Vision and Pattern Recognition*, pages 5356–5364, 2019. 1
- [13] Kaiming He, Ross Girshick, and Piotr Dollár. Rethinking imagenet pre-training. In *Proceedings of the IEEE international conference on computer vision*, pages 4918–4927, 2019. 7, 8
- [14] K. He, G. Gkioxari, P. Dollár, and R. Girshick. Mask r-cnn. In *2017 IEEE International Conference on Computer Vision (ICCV)*, pages 2980–2988, 2017. 1, 2, 3, 4, 7
- [15] Kaiming He, Xiangyu Zhang, Shaoqing Ren, and Jian Sun. Deep residual learning for image recognition. In *Proceedings of the IEEE conference on computer vision and pattern recognition*, pages 770–778, 2016. 4, 5
- [16] Cheng-Chun Hsu, Kuang-Jui Hsu, Chung-Chi Tsai, Yen-Yu Lin, and Yung-Yu Chuang. Weakly supervised instance segmentation using the bounding box tightness prior. In H. Wallach, H. Larochelle, A. Beygelzimer, F. d’Alché-Buc, E. Fox, and R. Garnett, editors, *Advances in Neural Information Processing Systems*, volume 32, pages 6586–6597. Curran Associates, Inc., 2019. 3
- [17] Ronghang Hu, Piotr Dollár, Kaiming He, Trevor Darrell, and Ross Girshick. Learning to segment every thing. In *Proceedings of the IEEE Conference on Computer Vision and Pattern Recognition*, pages 4233–4241, 2018. 1, 2, 7
- [18] Sergey Ioffe and Christian Szegedy. Batch normalization: Accelerating deep network training by reducing internal covariate shift. volume 37 of *Proceedings of Machine Learning Research*, pages 448–456, Lille, France, 07–09 Jul 2015. PMLR. 4
- [19] Anna Khoreva, Rodrigo Benenson, Jan Hosang, Matthias Hein, and Bernt Schiele. Simple does it: Weakly supervised instance and semantic segmentation. In *Proceedings of the IEEE Conference on Computer Vision and Pattern Recognition (CVPR)*, July 2017. 3
- [20] Weicheng Kuo, Anelia Angelova, Jitendra Malik, and Tsung-Yi Lin. Shapemask: Learning to segment novel objects by refining shape priors. In *The IEEE International Conference on Computer Vision (ICCV)*, October 2019. 1, 2, 3, 6, 7
- [21] Issam H Laradji, David Vazquez, and Mark Schmidt. Where are the masks: Instance segmentation with image-level supervision. *BMVC*, 2019. 3
- [22] Youngwan Lee and Jongyoul Park. Centermask: Real-time anchor-free instance segmentation. In *CVPR*, 2020. 1, 2
- [23] Tsung-Yi Lin, Piotr Dollar, Ross Girshick, Kaiming He, Bharath Hariharan, and Serge Belongie. Feature pyramid networks for object detection. In *Proceedings of the IEEE Conference on Computer Vision and Pattern Recognition (CVPR)*, July 2017. 4, 5
- [24] Tsung-Yi Lin, Michael Maire, Serge Belongie, James Hays, Pietro Perona, Deva Ramanan, Piotr Dollár, and C. Lawrence Zitnick. Microsoft coco: Common objects in context. In David Fleet, Tomas Pajdla, Bernt Schiele, and Tinne Tuytelaars, editors, *Computer Vision – ECCV 2014*, pages 740–755, Cham, 2014. Springer International Publishing. 1, 2, 5

- [25] Shu Liu, Jiaya Jia, Sanja Fidler, and Raquel Urtasun. Sgn: Sequential grouping networks for instance segmentation. In *Proceedings of the IEEE International Conference on Computer Vision*, pages 3496–3504, 2017. 2
- [26] Shu Liu, Lu Qi, Haifang Qin, Jianping Shi, and Jiaya Jia. Path aggregation network for instance segmentation. In *Proceedings of IEEE Conference on Computer Vision and Pattern Recognition (CVPR)*, 2018. 1, 2
- [27] Diego Marcos, Devis Tuia, Benjamin Kellenberger, Lisa Zhang, Min Bai, Renjie Liao, and Raquel Urtasun. Learning deep structured active contours end-to-end. In *Proceedings of the IEEE Conference on Computer Vision and Pattern Recognition*, pages 8877–8885, 2018. 2
- [28] Davy Neven, Bert De Brabandere, Marc Proesmans, and Luc Van Gool. Instance segmentation by jointly optimizing spatial embeddings and clustering bandwidth. In *Proceedings of the IEEE Conference on Computer Vision and Pattern Recognition*, pages 8837–8845, 2019. 2
- [29] Adam Paszke, Sam Gross, Francisco Massa, Adam Lerer, James Bradbury, Gregory Chanan, Trevor Killeen, Zeming Lin, Natalia Gimelshein, Luca Antiga, Alban Desmaison, Andreas Kopf, Edward Yang, Zachary DeVito, Martin Raison, Alykhan Tejani, Sasank Chilamkurthy, Benoit Steiner, Lu Fang, Junjie Bai, and Soumith Chintala. Pytorch: An imperative style, high-performance deep learning library. In H. Wallach, H. Larochelle, A. Beygelzimer, F. d'Alché-Buc, E. Fox, and R. Garnett, editors, *Advances in Neural Information Processing Systems 32*, pages 8024–8035. Curran Associates, Inc., 2019. 5
- [30] Sida Peng, Wen Jiang, Huaijin Pi, Xiuli Li, Hujun Bao, and Xiaowei Zhou. Deep snake for real-time instance segmentation. In *IEEE/CVF Conference on Computer Vision and Pattern Recognition (CVPR)*, June 2020. 1, 2
- [31] Shaoqing Ren, Kaiming He, Ross Girshick, and Jian Sun. Faster r-cnn: Towards real-time object detection with region proposal networks. In C. Cortes, N. D. Lawrence, D. D. Lee, M. Sugiyama, and R. Garnett, editors, *Advances in Neural Information Processing Systems 28*, pages 91–99. Curran Associates, Inc., 2015. 2
- [32] Carsten Rother, Vladimir Kolmogorov, and Andrew Blake. Grabcut -interactive foreground extraction using iterated graph cuts. *ACM Transactions on Graphics (SIGGRAPH)*, August 2004. 3
- [33] Syed Waqas Zamir, Aditya Arora, Akshita Gupta, Salman Khan, Guolei Sun, Fahad Shahbaz Khan, Fan Zhu, Ling Shao, Gui-Song Xia, and Xiang Bai. isaid: A large-scale dataset for instance segmentation in aerial images. In *Proceedings of the IEEE Conference on Computer Vision and Pattern Recognition Workshops*, pages 28–37, 2019. 1
- [34] Yuxin Wu, Alexander Kirillov, Francisco Massa, Wan-Yen Lo, and Ross Girshick. Detectron2. <https://github.com/facebookresearch/detectron2>, 2019. 5, 7, 8
- [35] Wenqiang Xu, Haiyang Wang, Fubo Qi, and Cewu Lu. Explicit shape encoding for real-time instance segmentation. In *Proceedings of the IEEE International Conference on Computer Vision*, pages 5168–5177, 2019. 2
- [36] Rufeng Zhang, Zhi Tian, Chunhua Shen, Mingyu You, and Youliang Yan. Mask encoding for single shot instance segmentation. In *Proceedings of the IEEE/CVF Conference on Computer Vision and Pattern Recognition (CVPR)*, June 2020. 8
- [37] B. Zhou, A. Khosla, Lapedriza. A., A. Oliva, and A. Torralba. Learning Deep Features for Discriminative Localization. *CVPR*, 2016. 2, 4
- [38] Yanzhao Zhou, Xin Wang, Jianbin Jiao, Trevor Darrell, and Fisher Yu. Learning saliency propagation for semi-supervised instance segmentation. In *Proceedings of the IEEE/CVF Conference on Computer Vision and Pattern Recognition*, pages 10307–10316, 2020. 1, 2, 3, 6, 7
- [39] Yanzhao Zhou, Yi Zhu, Qixiang Ye, Qiang Qiu, and Jianbin Jiao. Weakly supervised instance segmentation using class peak response. In *Proceedings of the IEEE Conference on Computer Vision and Pattern Recognition*, pages 3791–3800, 2018. 3
- [40] Yi Zhu, Yanzhao Zhou, Huijuan Xu, Qixiang Ye, David Doremann, and Jianbin Jiao. Learning instance activation maps for weakly supervised instance segmentation. In *Proceedings of the IEEE Conference on Computer Vision and Pattern Recognition*, pages 3116–3125, 2019. 3



Figure 8: Qualitative results on COCO using the non-voc  $\rightarrow$  voc split for training. This shows the ability of OPMask to predict precise instance masks for novel objects across different scenes, and various object sizes and appearances.

## Appendix

### A. Implementation & Training Details

**Input.** For input augmentations during training we use image resizing and horizontal flipping. Each input image is randomly flipped with a probability of 0.5 and resized such that its shorter side corresponds to a random value in (640, 672, 704, 736, 768, 800). If after resizing the longer image side exceeds 1333 pixels, the image is resized again so that the longer side equals 1333 pixels. During evaluation, the shorter image side is set to 800 pixels, while the maximum side remains at 1333 pixels.

**Optimization.** We train OPMask end-to-end following the multi-task loss definition of a Mask R-CNN combining box classification, box regression, RPN and mask prediction loss with equal weights:

$$\mathcal{L} = \mathcal{L}_{Cls} + \mathcal{L}_{Reg} + \mathcal{L}_{RPN} + \mathcal{L}_{Mask}. \quad (5)$$

For instances without mask labels  $\mathcal{L}_{Mask}$  is omitted.

### B. Additional Qualitative Results

In Figure 8 we present additional COCO images with overlaid mask predictions. While Figure 5 shows the voc  $\rightarrow$  non-voc setting, these results are produced in the non-

voc  $\rightarrow$  voc setting. Again, the results show OPMask’s ability to generate precise predictions for novel objects across different scenarios and object sizes. As before we use OPMask with a ResNet-101 backbone.